



## Grid connected inverter with SVPWM technique for photovoltaic application

A. Chitra<sup>1</sup>, K.Giridharan<sup>1</sup> and C. Chellamuthu<sup>2</sup>

<sup>1</sup>School of Electrical Engineering, VIT University, Vellore-632014.

<sup>2</sup>Department of Electrical and Electronics Engineering, R.M.K. Engineering College, R.S.M. Nagar, Kavaraipettai- 601206.

### ARTICLE INFO

#### Article history:

Received: 22 August 2011;

Received in revised form:

26 August 2011;

Accepted: 31 August 2011;

#### Keywords

Two level inverter,  
Photovoltaic array,  
SVPWM,  
MPPT.

### ABSTRACT

The global electrical energy consumption is rising and there is a steady increase of the demand on the power capacity, efficient production, distribution and utilization of energy. Power electronics, the technology of efficiently processing electric power, play an essential part in the integration of the dispersed generating stations for higher efficiency and better performance of the power systems. This project deals with the simulation of grid connected inverter for Photovoltaic applications. Space vector pulse width modulation (SVPWM) technique has been adopted for generating pulses for the two level inverter. The entire system comprising of Photovoltaic array (PVA) and two level inverter has been developed in Mat lab-Simulink. The PVA model characteristics including the effects of temperature and solar irradiation change on maximum power point are also presented in this paper. The inverter output has been synchronized with the grid using d-q theory and the power flow is controlled at 200kw. Finally, the inverter has been tested in grid connected mode.

© 2011 Elixir All rights reserved.

### Introduction

A huge problem that many countries around the world are facing is energy generation and pollution has a very large influence in that. The air quality has become very low in some areas. The more carbon dioxide we pump into the atmosphere, the greater the effect of air pollution and global warming becomes. Fossil fuels are fast depleting and as they are the major component used in energy production, we have to think of an efficient method of producing energy. This method of energy production should not be dependent on fossil fuels and should not produce any harmful by-products. As India is a vast tropical country the solar energy is abundantly available. So we can use the solar energy to produce electrical energy. This will not only prove to be cheap in the long run but will also help us face current energy challenges.

Globally, solar energy will be an increasingly important part of power generation in the new millennium. By making the solar energy easy to use and economically profitable, we can reduce the use of the fossil fuels.

Even though there are many other renewable sources of energy (wind, hydro, geo-thermal, tidal etc) importance is given to solar or PV systems because they are ideally suited for distributed resource applications.

Distributed resources are generation sources that can be located at or near loads. The PV arrays can give us cost effective solution for industrial and domestic applications. The inverters used for PV/grid systems, convert the DC voltage generated at the PV array to a suitable AC voltage. The PV industry has the need of more sophisticated inverter design to enhance their functionality, reduce cost and suit to new proposed topologies.

### Two Level Inverter

The inverter is composed of six group of active switches, S1 ~ S6, with a free-wheeling diode in parallel with each switch. Depending on the dc operating voltage of the inverter, each switch group consists of two or more IGBT or GCT switching devices connected in series.

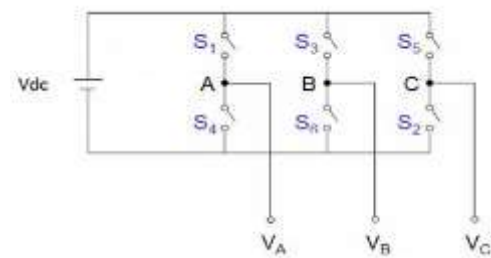


**Figure 1 Two-Level voltage source inverter  
Space vector pulse width modulation  
Switching States**

The operating status of the switches in the two-level inverter in Figure 1 can be represented by switching states. As indicated in Table 1, switching state 'P' denotes that the upper switch in an inverter leg is on and the inverter terminal voltage ( $v_{an}$ ,  $v_{bn}$ , or  $v_{cn}$ ) is positive ( $+V_d$ ) while 'O' indicates that the inverter terminal voltage is zero due to the conduction of the lower switch. There are eight possible combinations of switching states in the two-level inverter as listed in Table 1. The switching state [POO], for example, corresponds to the conduction of S1, S6, and S2 in the inverter legs A, B, and C, respectively. Among the eight switching states, [PPP] and [OOO] are zero states and the others are active states.

### Space vectors

The active and zero switching states can be represented by active and zero space vectors, respectively. A typical space vector diagram for the two-level inverter is shown in Table 1 where the six active vectors V1 to V6 form a regular hexagon with six equal sectors (I to VI). The zero vector V0 lies on the center of the hexagon.

To derive the relationship between the space vectors and switching states, refer to the two-level inverter in Figure 1. Assuming that the operation of the inverter is three-phase balanced, equation (1) gives

$$V_{Ao}(t) + V_{Bo}(t) + V_{Co}(t) = 0 \quad (1)$$

where  $V_{Ao}$ ,  $V_{Bo}$ , and  $V_{Co}$  are the instantaneous load phase voltages. From mathematical point of view, one of the phase voltages is redundant since given any two phase voltages, the third one can be readily calculated. Therefore, it is possible to transform the three-phase variables to equivalent two-phase variables as in equation (2).

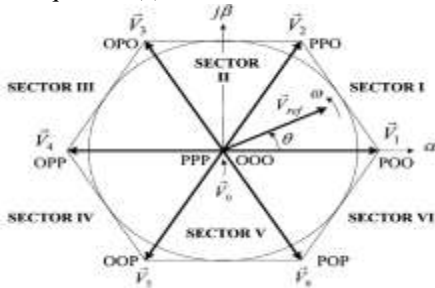


Figure 3 space vector diagram for two level inverter

$$\begin{bmatrix} v_{\alpha}(t) \\ v_{\beta}(t) \end{bmatrix} = \frac{2}{3} \begin{bmatrix} 1 & \frac{1}{2} & \frac{1}{2} \\ 0 & \frac{\sqrt{3}}{2} & -\frac{\sqrt{3}}{2} \end{bmatrix} \begin{bmatrix} V_{Ao}(t) \\ V_{Bo}(t) \\ V_{Co}(t) \end{bmatrix} \tag{2}$$

The coefficient  $2/3$  is somewhat arbitrarily chosen. The commonly used value is  $2/3$  or  $\sqrt{\frac{2}{3}}$ . The main advantage of

using  $2/3$  is that the magnitude of the two-phase voltages will be equal to that of the three-phase voltages after the transformation. A space vector can be generally expressed in terms of the two-phase voltages in the  $\alpha$ - $\beta$  plane as in equation (3)

$$V(t) = V_{\alpha}(t) + jV_{\beta}(t) \tag{3}$$

Substituting (2) in to (3), we have

$$V(t) = \frac{2}{3} [V_{Ao}(t)e^{j0} + V_{Bo}(t)e^{j\frac{2\pi}{3}} + V_{Co}(t)e^{j\frac{4\pi}{3}}] \tag{4}$$

where  $e^{jx} = \cos x + jsinx$  and  $x = 0, 2\pi/3$  or  $4\pi/3$ .

For active switching state [POO], the generated load phase voltages are substituted in the equation (4) in order to obtain the corresponding space vector as in equation (5).

$$V_1 = \left(\frac{2}{3}\right) V_{\alpha} e^{j0} \tag{5}$$

Following the same procedure, all the six active vectors can be derived as in equation (6)

$$V_k = \left(\frac{2}{3}\right) V_{\alpha} e^{j\frac{(k-1)\pi}{3}}, k=1,2,..,6 \tag{6}$$

The zero vector  $V_0$  has two switching states [PPP] and [OOO], one of which seems redundant. As will be seen later, the redundant switching state can be utilized to minimize the switching frequency of the inverter or perform other useful functions. It is to be noted that the zero and active vectors do not move in space, and thus they are referred to as stationary vectors. On the contrary, the reference vector  $V_{ref}$  in Figure 1 rotates in space at an angular velocity

$$\omega = 2\pi f_1 \tag{7}$$

where  $f_1$  is the fundamental frequency of the inverter output voltage. The angular displacement between  $V_{ref}$  and the  $\alpha$ -axis of the  $\alpha$ - $\beta$  plane can be obtained by

$$\theta(t) = \int_0^t \omega(t) dt + \theta(0) \tag{8}$$

For a given magnitude (length) and position,  $V_{ref}$  can be synthesized by three near by stationary vectors, based on which the switching states of the inverter can be selected and gate

signals for the active switches can be generated. When  $V_{ref}$  passes through sectors one by one, different sets of switches will be turned on or off. As a result, when  $V_{ref}$  rotates one revolution in space, the inverter output voltage varies one cycle over time. The inverter output frequency corresponds to the rotating speed of  $V_{ref}$ , while its output voltage can be adjusted by the magnitude of  $V_{ref}$ .

**PVA Modeling**

PV arrays are built up with combined series/parallel combinations of PV solar cells, which are usually represented by a simplified equivalent circuit model such as the one given in Figure 4 and / or by an equation as in (9)

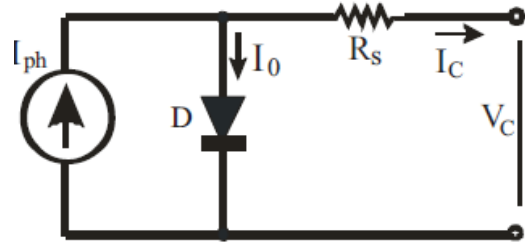


Figure 4 simplified equivalent circuit of photovoltaic cell

The PV cell output voltage is a function of the photocurrent that mainly determined by load current depending on the solar irradiation level during the operation as in equation (9).

$$V_c = \frac{AKTc}{e} \ln \left[ \frac{I_{ph} + I_0 - I_c}{I_0} \right] R_s I_c \tag{9}$$

where the symbols are defined as follows:

e: electron charge ( $1.602 \times 10^{-19}$  C).

k: Boltzmann constant ( $1.38 \times 10^{-23}$  J/oK).

Ic: cell output current, A.

Iph: photocurrent, function of irradiation level and junction temperature (5 A).

I0: reverse saturation current of diode(0.0002A).

Rs: series resistance of cell (0.001  $\Omega$ ).

Tc: reference cell operating temperature (20  $^{\circ}$ C).

Vc: cell output voltage, V.

Both k and Tc should have the same temperature unit, either Kelvin or Celsius. The curve fitting factor A is used to adjust the I-V characteristics of the cell to the actual characteristics obtained by testing. Eq. (9) gives the voltage of a single solar cell which is then multiplied by the number of the cells connected in series to calculate the full array voltage. Since the array current is the sum of the currents flowing through the cells in parallel branches, the cell current Ic is obtained by dividing the array current by the number of the cells connected in parallel before being used in (9), which is only valid for a certain cell operating temperature Tc with its corresponding solar irradiation level Sc. If the temperature and solar irradiation levels change, the voltage and current outputs of the PV array will follow this change. Hence, the effects of the changes in temperature and solar irradiation levels should also be included in the final PV array model. A method to include these effects in the PV array modeling is given by Buresch [1]. According to his method, for a known temperature and a known solar irradiation level, a model is obtained and then this model is modified to handle different cases of temperature and irradiation levels. Let (9) be the benchmark model for the known operating temperature Tc and known solar irradiation level Sc as given in the specification. When the ambient temperature and irradiation levels change, the cell operating temperature also changes, resulting in a new output voltage and a new photocurrent value.

The solar cell operating temperature varies as a function of solar irradiation level and ambient temperature. The variable ambient temperature  $T_a$  affects the cell output voltage and cell photocurrent. These effects are represented in the model by the temperature coefficients  $C_{TV}$  and  $C_{TI}$  for cell output voltage and cell photocurrent, respectively, as in equations (10- , 11):

$$C_{TV} = 1 + \beta_T (T_a - T_x) \tag{10}$$

$$C_{TI} = 1 + \frac{Y_t}{S_c} (T_x - T_a) \tag{11}$$

where,  $\beta_T = 0.004$  and  $Y_t = 0.06$  for the cell used and  $T_a = 20$  degree centigrade is the ambient temperature during the cell testing. This is used to obtain the modified model of the cell for another ambient temperature  $T_x$ . Even if the ambient temperature does not change significantly during the daytime, the solar irradiation level changes depending on the amount of sunlight and clouds. A change in solar irradiation level causes a change in the cell photocurrent and operating temperature, which in turn affects the cell output voltage. If the solar irradiation level increases from  $S_{x1}$  to  $S_{x2}$ , the cell operating temperature and the photocurrent will also increase from  $T_{x1}$  to  $T_{x2}$  and from  $I_{ph1}$  to  $I_{ph2}$ , respectively. Thus the change in the operating temperature and in the photocurrent due to variation in the solar irradiation level can be expressed via two constants, CSV and CSI, which are the correction factors for changes in cell output voltage  $V_C$  and photocurrent  $I_{ph}$ , respectively as in equations (12-13):

$$C_{SV} = 1 + \beta_T \alpha_s (S_x - S_c) \tag{12}$$

$$C_{SI} = 1 + \frac{1}{S_c} (S_x - S_c) \tag{13}$$

where  $S_c$  is the benchmark reference solar irradiation level during the cell testing to obtain the modified cell model.  $S_x$  is the new level of the solar irradiation. The temperature change,  $\Delta T_c$ , occurs due to the change in the solar irradiation level and is obtained using equation (14)

$$\Delta T_c = \alpha_s (S_x - S_c) \tag{14}$$

The constant  $\alpha_s$  represents the slope of the change in the cell operating temperature due to a change in the solar irradiation level [1] and is equal to 0.2 for the solar cells used. Using correction factors  $C_{TV}$ ,  $C_{TI}$ ,  $C_{SV}$  and  $C_{SI}$ , the new values of the cell output voltage  $V_{CX}$  and photocurrent  $I_{phx}$  are obtained for the new temperature  $T_x$  and solar irradiation  $S_x$  as in equations (15-16):

$$V_{CX} = C_{TV} C_{SV} V_C \tag{15}$$

$$I_{phx} = C_{TI} C_{SI} I_{ph} \tag{16}$$

$V_C$  and  $I_{ph}$  are the benchmark reference cell output voltage and reference cell photocurrent, respectively. The resulting I-V and P-V curves for various temperature and solar irradiation are shown in the results.

**Maximum Power Point Tracking**

The P&O algorithms operate by periodically perturbing (i.e. incrementing or decrementing) the array terminal voltage or current and comparing the PV output power with that of the previous perturbation cycle. If the PV array operating voltage changes and power increases ( $dP/dVPV > 0$ ), the control system moves the PV array operating point in that direction; otherwise the operating point is moved in the opposite direction. In the next perturbation cycle the algorithm continues in same way. A

common problem in P&O algorithms is that the array terminal voltage is perturbed every MPPT cycle; therefore when the MPP is reached, the output power oscillates around the maximum, resulting in power loss in the PV system. This is especially true in constant or slowly-varying atmospheric conditions. P&O methods can fail under rapidly changing atmospheric conditions (see Figure 9). Starting from an operating point A, if atmospheric conditions stay approximately constant, a perturbation  $\Delta V$  the voltage  $V$  will bring the operating point to B and the perturbation will be reversed due to a decrease in power. However, if the irradiance increases and shifts the power curve from  $P_1$  to  $P_2$  within one sampling period, the operating point will move from A to C. This represents an increase in power and the perturbation is kept the same. Consequently, the operating point diverges from the MPP and will keep diverging if the irradiance steadily increases.

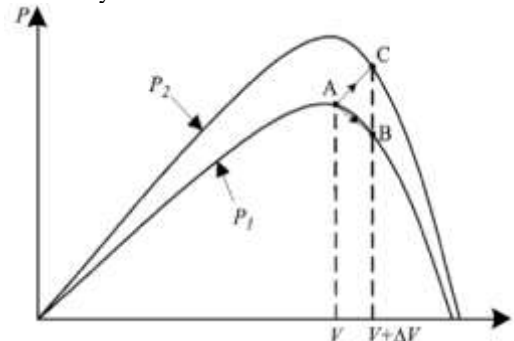


Figure 5 Divergence of P&O

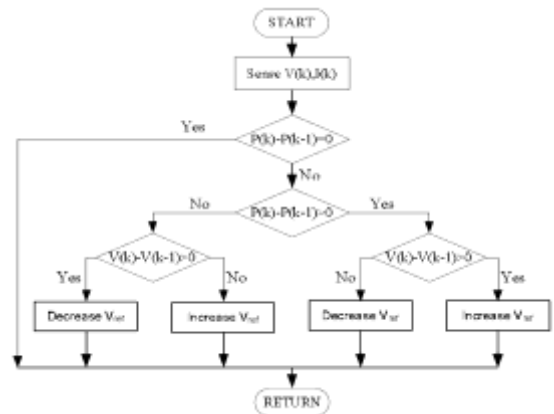


Figure 6 Flow chart for P&O method Simulation of grid connected PV inverter

The primary function of a voltage source inverter (VSI) is to convert a fixed dc voltage to a three-phase ac voltage with variable magnitude and frequency. in the Figure 1 shows that the block diagram of two level voltage source inverter, with space vector pulse width modulation technique is used to generate a pulses to the inverter.

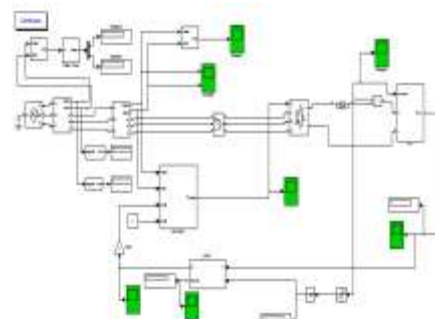


Figure 7. P V Array model

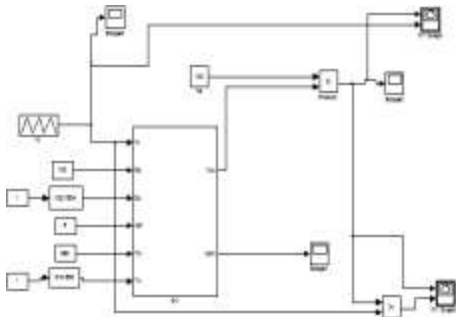


Figure 8 Simulation of PVA model

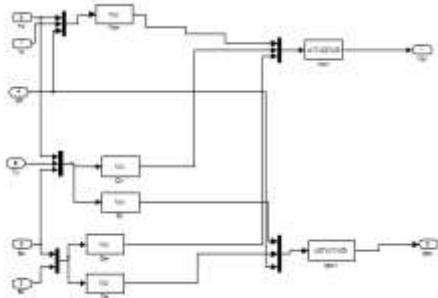


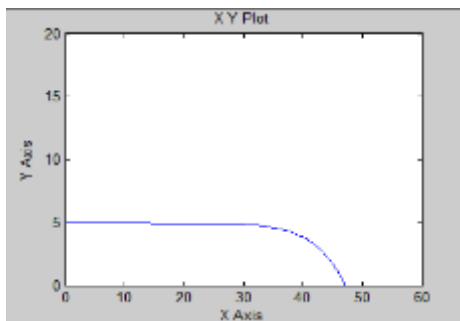
Figure 9 Subsystem of PVA Model

**Simulation Results**

The proposed PVA model is simulated using the scheme given in Figure 4. The PVA modeling and space vector modulation technique for two level inverter is included in this paper. The current-voltage (I-V) characteristic of the PVA during operation is given in Figure 10.

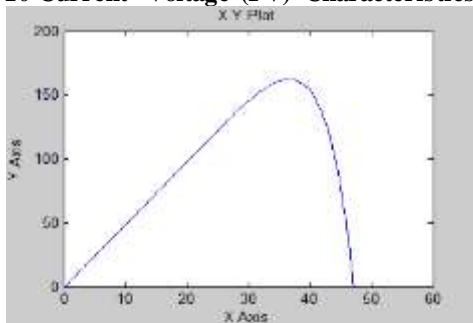
Since the voltage of the PVA is equal to the open circuit voltage at stand-still, the I-V characteristics start at open circuit voltage with current equal to zero.

As the simulation starts and the loads begin draw current from the PVA, the voltage and the current start moving toward the operating values, which are shown in Figure 10 for voltage and current, respectively. PVA power - voltage is given in Figure 11.



PVA VOLTAGE (V)

Figure 10 Current- Voltage (I-V) Characteristics of PVA



PVA VOLTAGE (V)

Figure 11 Power-Voltage Characteristics of PVA

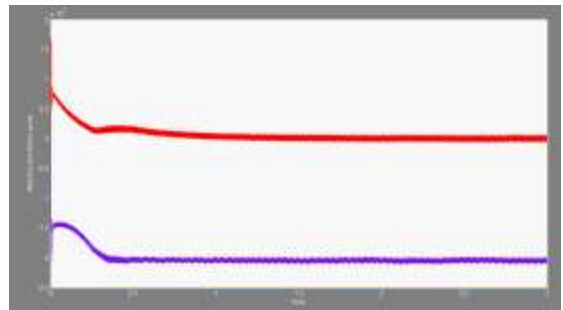


Figure 12 Reactive and Active Power

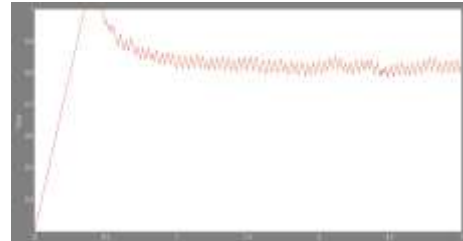


Figure 13 MPPT output

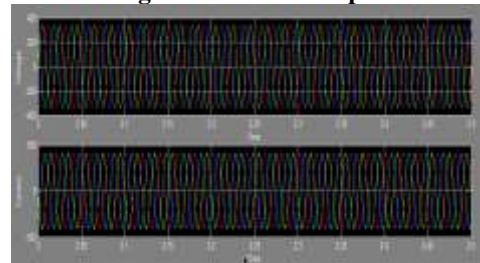


Figure 14 Voltage and Current Outputs at Grid Side Conclusion

In this paper space vector pulse width modulation (SVPWM) technique has been adopted for generating pulses for the two level inverter. The entire system comprising of Photovoltaic array (PVA) and two level inverter has been developed in Matlab-Simulink. The PVA model characteristics including the effects of temperature and solar irradiation change on maximum power point are also presented in this paper. The inverter output has been synchronized with the grid using d-q theory. The active power control is done at 200KW as shown in Figure 12. Finally, the inverter has been tested in grid connected mode.

**References**

- [1]. M. Buresch: *Photovoltaic Energy Systems Design and Installation*, McGraw-Hill, New York, 1983.
- [2]. Z. M. Salameh and F. Dagher: *The effect of electrical array reconfiguration on the performance of a PV powered volumetric water pump*, IEEE Trans., EC-5 (1990) 653-658.
- [3]. I. H. Altas and A. M. Sharaf: *A Fuzzy Logic Power Tracking Controller For A Photovoltaic Energy Conversion Scheme*, Electric Power Systems Research Journal, Vol.25, No.3, pp.227-238, 1992.
- [4]. M.A.S Masoum, And H. Dehbonei: *Design, Construction and Testing of a Voltage-based Maximum Power Point Tracker (VMPP) for Small Satellite Power Supply*, 13th Annual AIAA/USU Conference on Small Satellites, pp.1-12., 1999.
- [5]. Y-C. Kuo, T-J. Liang, and J-F. Chen: *Novel Maximum-Power-Point- Tracking Controller for Photovoltaic Energy Conversion System*, IEEE Transactions On Industrial Electronics, Vol. 48, No. 3, June 2001, Pp.594-601.
- [6]. T. Noguchi, S. Togashi, and R. Nakamoto: *Short-Current Pulse-Based Maximum-Power-Point Tracking Method for Multiple Photovoltaic and Converter Module System*, IEEE

Transactions On Industrial Electronics, Vol. 49, No. 1, February 2002, 217-223.

[7]. M. A. S. Masoum, H. Dehbonei, and E. F. Fuchs., *Theoretical and Experimental Analyses of Photovoltaic Systems With Voltage- and Current-Based Maximum Power-Point Tracking*, IEEE Transactions On Energy Conversion, Vol. 17, No. 4, December 2002, Pp.514-522.

[8]. Hua and J. Lin: *An on-line MPPT algorithm for rapidly changing illuminations of solar arrays*, Renewable Energy 28 (2003) 1129–1142.

[9]. K. Benlarbi, L. Mokrani, M.S. Nait-Said: *A fuzzy global efficiency optimization of a photovoltaic water pumping system*, Solar Energy, 77 (2004) 203–216.

[10]. Hua and J. Lin: *A modified tracking algorithm for maximum power tracking of solar array*, Energy Conversion and Management, 45 (2004) 911–925.

[11]. Y-M. Chen, Y-C. Liu, and F-Y. Wu: *Multi input Converter With Power Factor Correction, Maximum Power Point*

*Tracking, and Ripple-Free Input Currents*, IEEE Transactions On Power Electronics, Vol. 19, No. 3, May 2004, pp.631-639.

[12]. Matlab and Simulink, The Mathworks, Inc. as of September 2000 <http://www.mathworks.com>.

[13]. N. Mohan, T. M. Undeland, et al., *Power Electronics—Converters, Applications and Design*, 3rd edition, John Wiley & Sons, New York, 2003.

[14]. A. M. Hava, R. J. Kerkman, et al., *Carrier-based PWM-VSI Overmodulation Strategies: Analysis, Comparison and Design*, IEEE Transactions on Power Electronics, Vol. 13, No. 4, pp. 674–689, 1998.

[15]. D. G. Holmes and T. A. Lipo, *Pulse Width Modulation for Power Converters—Principle and Practice*, IEEE Press/Wiley-Interscience, New York, 2003.

[16]. M. H. Rashid, *Power Electronics Handbook*, Academic Press, New York, 2001.

[17]. P. C. Krause, O. Wasynczuk, et al., *Analysis of Electric Machinery and Drive Systems*, 2nd edition, IEEE Press/Wiley-Interscience, New York, 2002.

**Table 1 Definition of switching states**

Switching states	Leg A			Leg B			Leg C		
	S1	S4	Van	S3	S6	Vbn	S5	S2	Vbn
P	On	off	Vd	On	off	Vd	On	off	Vd
O	Off	on	0	Off	on	0	Off	on	0